

LEP1 HEAVY FLAVOUR ELECTROWEAK PHYSICS AND 2-FERMION PROCESSES AT LEP2

Thomas Schörner-Sadenius

*CERN, Division EP, 1211 Geneva 23, Switzerland and
Hamburg University, Luruper Chaussee 149, 22761 Hamburg, Germany*

Abstract

Results from heavy flavour electroweak physics at LEP1 are reviewed together with measurements of 2-fermion processes at LEP2. For the former measurements the emphasis is on analyses of heavy quark forward-backward asymmetries, $A_{FB}^{b,c}$, and on the partial decay widths of the Z^0 to heavy quarks, $R_{b,c}$. The measurements of the heavy quark asymmetries are used to extract the effective electroweak mixing angle for leptons, $\sin^2 \theta_{eff}^{lept}$. A 2.9σ discrepancy between measurements of this quantity from $A_1(SLD)$ and from A_{FB}^b is observed. The 2-fermion processes at LEP2 are used to place stringent limits on physics processes beyond the Standard Model. However, all measured quantities are in reasonable agreement with the Standard Model expectations, and all calculated limits are well above the highest LEP2 center-of-mass energies.

1 Overview

Although the LEP experiments finished data taking in 2000, the analysis efforts are still strong in all four collaborations. In this article I will give an overview of the status of two rather distinct experimental areas, namely the heavy flavour electroweak measurements at LEP1 and 2-fermion processes at LEP2. Whereas the former class of analyses basically serve as a test of the electroweak Standard Model, with the main interest on the extraction of the weak mixing angle $\sin^2 \theta_{eff}$, the LEP2 2-fermion measurements can be used for generating limits on models for new physics beyond the Standard Model.

This article is structured as follows: Section 2 is devoted to the LEP1 heavy flavour measurements. After a short overview of general issues and experimental techniques the results of the partial decay width and forward-backward asymmetry measurements for heavy quarks are shown. At the end of the section, an interpretation of these results in terms of the Standard Model, namely the electroweak mixing angle $\sin^2 \theta_{eff}$, is given. Section 3 reviews measurements of 2-fermion processes at LEP2. A large part of the section is devoted to the interpretation of the measurements in terms of new physics models, such as contact interactions, Z' bosons or low scale gravity in large extra dimensions. Section 4 concludes the paper and gives an outlook.

2 LEP1 Heavy Flavour Electroweak Physics

2.1 Introduction

Measurements of b and c quark final states at LEP allow detailed insights into the properties of the electroweak Standard Model. The measurements considered here are a) the heavy flavour partial decay widths of the Z^0 , R_b and R_c , and b) the heavy quark forward-backward asymmetries, A_{FB}^b and A_{FB}^c .

R_q is defined as the decay width of the Z^0 to quarks of flavour q, normalized to the total hadronic decay width, and is proportional to the sum of the squared vector and axial vector couplings of the Z^0 :

$$R_q := \frac{\Gamma^q}{\Gamma_{had}} \propto g_{Vq}^2 + g_{Aq}^2, \quad (1)$$

R_q is therefore sensitive to vertex corrections to the $q\bar{q}Z^0$ vertex and might thus serve to detect signs of new physics modifying these vertices. Conceptually the measurement of $R_{b,c}$ is simple: One has to count the number of events with $b\bar{b}$ or $c\bar{c}$ final states and normalize to the number of all hadronic final state events. So the largest challenge, besides understanding the rather involved systematic uncertainties, is providing an efficient, clean and well-understood b or c flavour tag.

The forward-backward asymmetry measurements are more complicated. The asymmetry for flavour q is defined as

$$A_{FB}^q := \frac{N_F^q - N_B^q}{N_F^q + N_B^q} \quad (2)$$

where N_F^q (N_B^q) is the number of events of flavour q in which the initial quark goes into the forward (backward) hemisphere. The forward hemisphere is defined by the electron beam direction. Since at the Z^0 pole

$$A_{FB}^{q,0} = \frac{3}{4} \mathcal{A}_e \mathcal{A}_b \quad (3)$$

with

$$\mathcal{A}_f = 2 \frac{g_{Vf} \cdot g_{Af}}{g_{Vf}^2 + g_{Af}^2} \quad (4)$$

the asymmetries provide direct access to the electroweak mixing angle $\sin^2 \theta_{eff}$ via the relation $g_V/g_A = 1 - 4Q \cdot \sin^2 \theta_{eff}$. Due to the charge factor Q in the former relation, the sensitivity of the asymmetries to the heavy quark couplings \mathcal{A}_q is much reduced with respect to the electron coupling \mathcal{A}_e (even more for b than for c quarks). So the measurements serve in fact as a determination of the mixing angle for electrons (or leptons, assuming lepton universality), $\sin^2 \theta_{eff}^{lept}$.

The SLD e^+e^- collider, in contrast to LEP, has the possibility to polarize the electron beam so that additional measurements become available. One can for example, from a measurement of the left-right forward-backward asymmetry, A_{LRFB} , directly extract the heavy flavour couplings $\mathcal{A}_{b,c}$ which are not accessible at LEP. SLD measurements are also used in the heavy flavour fits that will be covered in the next sections.

The measurements of the partial decay widths ¹⁾ are final. The latest contributions to the forward-backward asymmetry measurements were presented at the 2002 summer conferences: OPAL prepared a new measurement of the b quark asymmetry using an inclusive charge tag ²⁾ which superseded their old result and substantially reduced the statistical and systematic uncertainties. DELPHI presented new preliminary measurements of the lepton-tagged b and c asymmetries ³⁾ which included new systematic studies. It is therefore fair to say that the LEP1 heavy flavour electroweak measurements are slowly coming to an end. The only missing pieces are a lepton-tag asymmetry measurement from OPAL and the inclusive b asymmetry measurement from DELPHI. In addition, some SLD measurements are also only preliminary (A_{LRFB} , R_c).

2.2 Tools: Flavour and Charge Tags

As became apparent in the previous section, the heavy flavour measurements rely on flavour tagging, and, in case of the asymmetry measurements, also

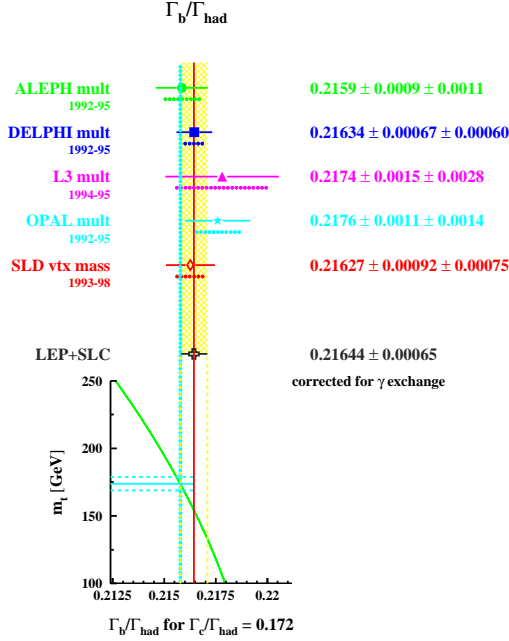


Figure 1: A compilation of measurements of R_b from LEP and SLD. Also the Standard Model expectation, which depends on the mass of the top quark m_t , is shown.

on tagging the charges of the outgoing quarks. The determination of these quantities is facilitated by the usually clear 2-jet structure of hadronic events at or around the Z^0 which allows the events to be divided in two hemispheres along the plane perpendicular to the thrust axis. The flavour and charge tagging tools can then be applied in the two hemispheres independently. Due to this basic structure nearly all information needed for the extraction of the partial decay widths and asymmetry values can be taken from the data without relying too much on Monte Carlo input.

Heavy flavour events can be tagged using heavy quark secondary decay vertices or high p_T leptons from semileptonic decays $b, c \rightarrow l$. The variables describing the decay vertices or the decay leptons are usually combined using likelihoods or artificial neural networks to result in one flavour tagging variable with high separation power between b or c quark hemispheres and the light flavour background, respectively. Purities of 95 % with efficiencies of 20 to 30 % can be reached. Another possibility is to tag c hemispheres using D^*

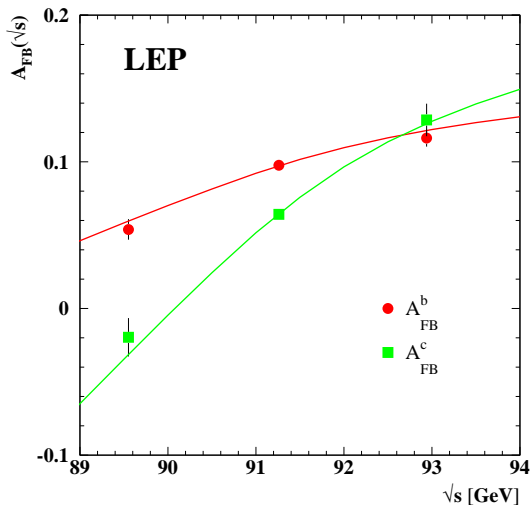


Figure 2: The b and c quark asymmetries as a function of the center-of-mass energy, compared to the ZFITTER Standard Model prediction.

mesons.

The charge of hemispheres which is needed for the forward-backward asymmetry analyses can be determined from a variety of observables. The OPAL analysis mentioned above uses the jet charge of the highest energy jet in the hemisphere, the weighted charge sum of all tracks connected to the secondary vertex in the hemisphere and, in addition, the charge of kaons originating from cascade decays $b \rightarrow c \rightarrow s$ measured using the dE/dx information from the OPAL central jet chamber. These variables are again combined in an artificial neural network. Charge tags like the one just described are self-calibrating in the sense that their efficiency and purity can be determined from the data themselves, thus reducing the dependence on external inputs from Monte Carlo simulations. It turns out that the correlation between the charge tags in the two event hemispheres is one of the dominant sources of systematic uncertainty.

In case of lepton-tagged asymmetry measurements, basically the same variables as for the flavour tag can be used: lepton momentum and transverse momentum, vertex fit probability, to mention a few, together with some charge information from the hemisphere opposite to the one with the identified lepton.

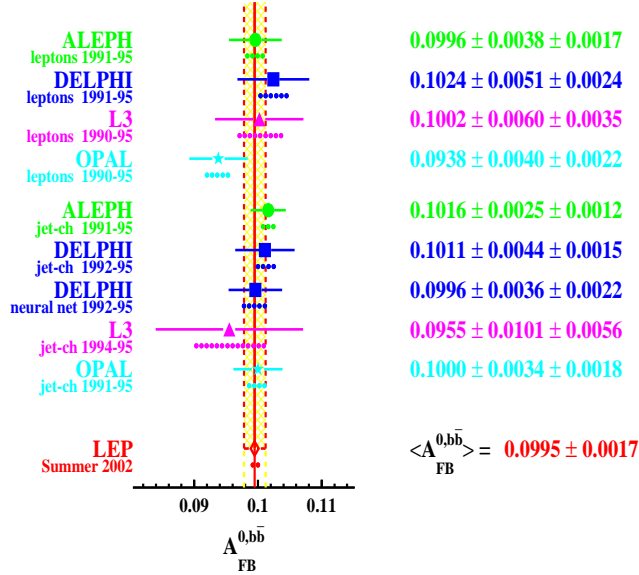


Figure 3: A compilation of $A_{FB}^{b,bb}$ measurements from LEP and SLD.

2.3 Results on Heavy Quark Decay Widths and Asymmetries

In order to get a more precise picture of heavy flavour electroweak physics, the various measurements of the partial decay widths and asymmetries are combined in a χ^2 minimisation procedure. In this fit, the correlations between various measurements due to mutual dependencies and to common external inputs are taken into account. Together with the LEP measurements of $R_{b,c}$ and $A_{FB}^{b,c}$ the SLD measurements of \mathcal{A}_b and \mathcal{A}_e are used in this fit. Some additional auxiliary parameters (charm hadron production fractions, b semileptonic branching ratios) are also determined.

Figure 1 shows a compilation of measurements of R_b together with the R_b result of the heavy flavour fit ¹⁾. The measurements of the four LEP experiments and of SLD are in good overall agreement. The fit results in a value $R_b = 0.21644 \pm 0.00065$. This value, indicated by the solid vertical line, is well compatible with the Standard Model prediction based on the best electroweak knowledge and the Tevatron top mass measurement (left vertical line). The various measurements of R_c are also averaged and result in a value of $R_c = 0.1717 \pm 0.0031$, again in good agreement with the theoretical expectation.

Turning to the asymmetry measurements, first all asymmetry measure-

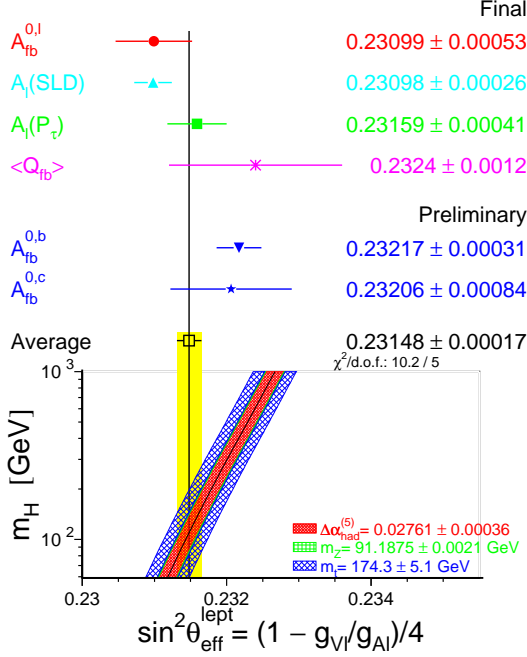


Figure 4: A compilation of measurements of the effective electroweak mixing angle for leptons, together with the LEP+SLD average.

ments are corrected to three distinct energies (the Z^0 pole and ± 2 GeV away from it), and the averaged asymmetry is extracted for these three energies separately. The result is shown in figure 2. Since the variation of the asymmetry with the center-of-mass energy is consistent with the Standard Model expectation, all asymmetry measurements are corrected to the Z^0 pole, corrected for photon radiation and quark mass effects, and combined. The contributing A_{FB}^b measurements (2, 3, 4, 5) and the derived global value of $A_{FB}^{b,0} = 0.0995 \pm 0.0015 \pm 0.0007$ are shown in figure 3. The average is dominated by the inclusive jet charge analyses from ALEPH, DELPHI and OPAL. For the c asymmetry (3, 5, 6) we find $A_{FB}^{c,0} = 0.0713 \pm 0.0031 \pm 0.0018$. In both cases the first error is statistical, and the second systematic. The common systematic uncertainty is 0.0004 (0.0009) for the b (c) asymmetry, resulting mainly from corrections due to gluon radiation.

2.4 Standard Model Interpretation

One can go one step further using some results of the heavy flavour electroweak fit described above (A_{FB}^b and A_{FB}^c), LEP combined measurements of the leptonic forward-backward asymmetry (A_{FB}^l and $\mathcal{A}_1(P_\tau)$) and the SLD \mathcal{A}_1 . Expressing all these quantities in terms of the vector and axial vector couplings of the Z^0 , g_V and g_A , one can extract the effective electroweak mixing angle for leptons, $\sin^2 \theta_{eff}^{lept}$.

As can be seen from figure 4, the resulting single values for this quantity fall roughly in two classes: the leptonic measurements (A_{FB}^l , $\mathcal{A}_1(P_\tau)$, $\mathcal{A}_1(SLD)$), which are dominated by the SLD number, tend to be slightly low, whereas the hadronic or inclusive results, in particular for A_{FB}^b , are rather high. The observed discrepancy of 2.9σ results in a χ^2 of $10.2/5$, corresponding to a 7 % probability.

The final $\sin^2 \theta_{eff}^{lept}$ value is 0.23148 ± 0.00017 , where the uncertainty is dominated by statistics. This combined value of the mixing angle, interpreted in the framework of the Standard Model, prefers a Higgs mass slightly above 100 GeV, whilst the A_{FB}^b measurements alone suggest a heavier Higgs of about 400 GeV.

3 2-Fermion Processes at LEP2

3.1 Introduction

The emphasis in measurements of 2-fermion processes at LEP2 is on searching for signs of new physics in the interference of new processes with the off-resonance Z^0/γ exchange. There are, however, a few general issues that have to be considered before deriving general results for 2-fermion processes. The most prominent problem is initial state radiation. Electron-positron annihilation events at center-of-mass energies above the Z^0 pole tend to radiate an energetic photon in the initial state, forcing the propagator back to the Z^0 mass. There is therefore a large contribution to the overall event sample at an effective center-of-mass energy corresponding to the Z^0 . These events, which do not contain any information not known from LEP1 physics, are rejected using a cut on the effective center-of-mass energy $\sqrt{s'}$ of the order of $0.85-0.9\sqrt{s}$. In addition to this complication, corrections have to be applied in order to compensate for different signal definitions and different treatments of ISR-FSR interference before the data of different experiments can be combined.

3.2 Measurements

The conceptually simplest measurement of 2-fermion processes is clearly that of the total cross-section as a function of the center-of-mass energy \sqrt{s} . After the

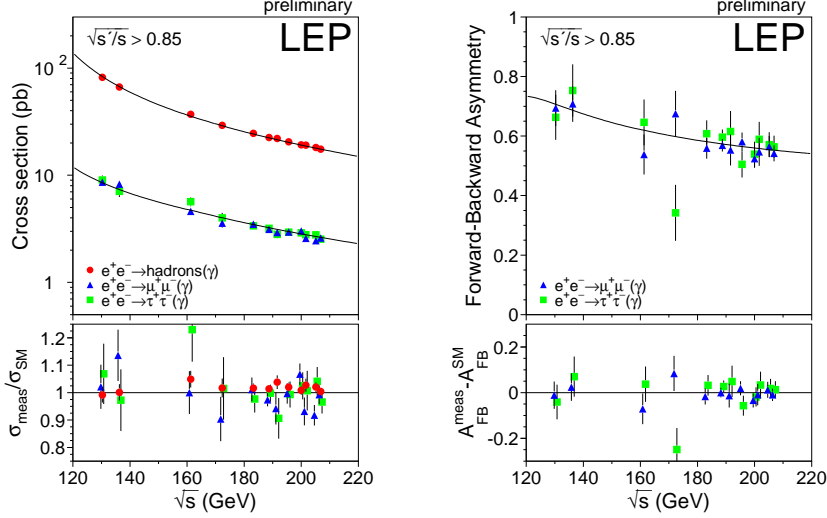


Figure 5: *The total cross-section and the forward-backward asymmetry for hadronic, μ and τ final states as a function of the center-of-mass energy, \sqrt{s} .*

above mentioned corrections have been applied, all measurements for quark, μ and τ final states from the four LEP collaborations are combined in a single χ^2 fit to give the average cross-sections (see ⁷⁾ and the LEP EW 2f subgroup web page ⁸⁾ for an overview on all measurements used). The results are shown as a function of \sqrt{s} in the left part of figure 5. The bottom part of the figure also shows the ratio of the data to the Standard Model expectation, indicating an overall good agreement for the leptonic channels. The hadronic measurements are slightly low (1.7σ). The overall χ^2 is 160/180. The same data are also used for the extraction of the forward-backward asymmetry; the result, again as a function of \sqrt{s} , is shown in the right half of figure 5. Here, the overall description of all data is satisfactory.

In a next step, differential cross-sections as a function of the scattering angle $\cos\theta$ are extracted for all three lepton generations in seven regions of the center-of-mass energy between 189 and 207 GeV. For the e^+e^- final states, the additional t channel contribution which is not present for the other lepton generations leads to a divergence of the cross-section towards $\cos\theta = 1$. The description of the data is satisfactory, except for the lowest bins for $\mu^+\mu^-$ and $\tau^+\tau^-$ final states at $\sqrt{s} = 202$ GeV. However, in these bins there are only low statistics, and for all other (lower and higher) energies this feature is not

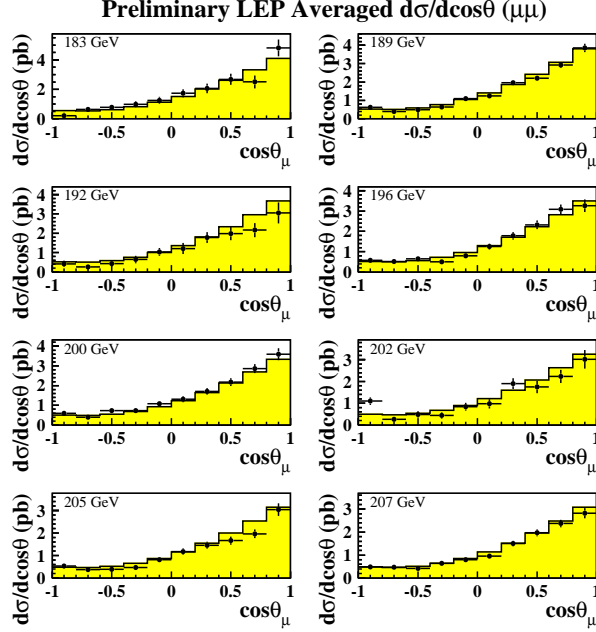


Figure 6: *Differential cross-section as a function of $\cos\theta$ for $e^+e^- \rightarrow \mu^+\mu^-$ for different center-of-mass energies. The data excess in the leftmost bin at 202 GeV is also present in the τ channel.*

present, see figure 6.

For heavy flavour quarks, the partial decay widths $R_q = \sigma_{q\bar{q}}/\sigma_{hadrons}$ and the forward-backward asymmetries are measured separately. For R_c , the only measurement is provided by ALEPH. The agreement between data and the ZFITTER Standard Model expectation is acceptable, except perhaps for R_b which tends to be low by about 2σ over all energies.

3.3 Interpretation in Non-standard Models

The data described above are interpreted in several physics models: electron-lepton and lepton-quark contact interactions, Z' bosons, and low scale gravity in large extra dimensions.

In the framework of contact interactions it is assumed that LEP2 has sensitivity to additional contributions to the Lagrangian which are parametrized

in the form

$$\mathcal{L}_{eff} = \frac{g^2}{(1 + \delta)\Lambda^2} \sum_{i,j=L,R} \eta_{ij} \bar{e}_i \gamma_\mu e_i \bar{f}_j \gamma^\mu f_j \quad (5)$$

with a coupling strength g for which usually $g^2/4\pi = 1$ is assumed, with Λ as the mass scale of the interaction, and with $\delta = 1$ (0) for $f = e$ ($f \neq e$). Also contained in the formula are the possibilities to define the helicity of the currents (L, R) and the sign of the interference of the new physics contributions with the Standard Model processes, $\eta_{ij} = \pm 1$. For the various models that can be built from this Lagrangian, the predictions are fitted to the measured total and/or differential cross-sections and asymmetries; the fitting parameter is defined as $\epsilon := 1/\Lambda^2$. The fitted ϵ values are converted into 95% confidence level limits on Λ which for all models are larger than 2.1 to 21.7 TeV, depending on the model. It is therefore fair to say that no signs for contact interactions have been found at LEP2. The left part of figure 7 shows an example for the limits in the μ plus τ channel for various models.

Z' bosons are an ingredient of several new physics models: In the E6 Grand Unified Theory, the group structure breaks down to the known Standard Model $SU(3)_c \times SU(2)_L \times U(1)_Y$, but additional $U(1)$ subgroups are also present which lead to Z' bosons. The Sequential Standard Model postulates the existence of a Z' boson with the same couplings as the standard Z boson¹. And in the so-called Left-Right Model, the existence of an additional $SU(2)_R$ subgroup would lead to Z' and W'^{\pm} bosons. The effect of the Z' can be parametrised as a contact term in the cross-section, so that the modified cross-section prediction can be fitted to the data, aiming for the extraction of the mass $M_{Z'}$ of the new boson. Depending on the model considered the derived limit for Z' bosons is found to be between 434 and 1787 GeV and therefore beyond the reach of LEP2.

Quantum gravity is a candidate for solving the hierarchy problem, i.e. for providing the missing link between the electroweak scale of order $\mathcal{O}(1 \text{ TeV})$ and the Planck scale $M_{Pl} = 10^{16} \text{ TeV}$. Assuming that quantum gravity lives in $4+n$ dimensions, whereas our Standard Model phenomenology is confined to the usual $3+1$ dimensions, it is possible that the $4+n$ quantum gravity pendant to the Planck scale is of the order of the electroweak scale. This new ‘Planck scale’ M_D would be related to the usual Planck scale M_{Pl} via

$$M_{Pl}^2 = M_D^{2+n} \cdot R^n \quad (6)$$

with R the size of the new additional dimensions. The effect of quantum gravity would be the exchange of virtual gravitons, a process which would interfere with

¹The mixing between the Z and the Z' is found to be consistent with 0, as is expected from LEP1 where no sign of Z' was found in the precision measurements of the Z .

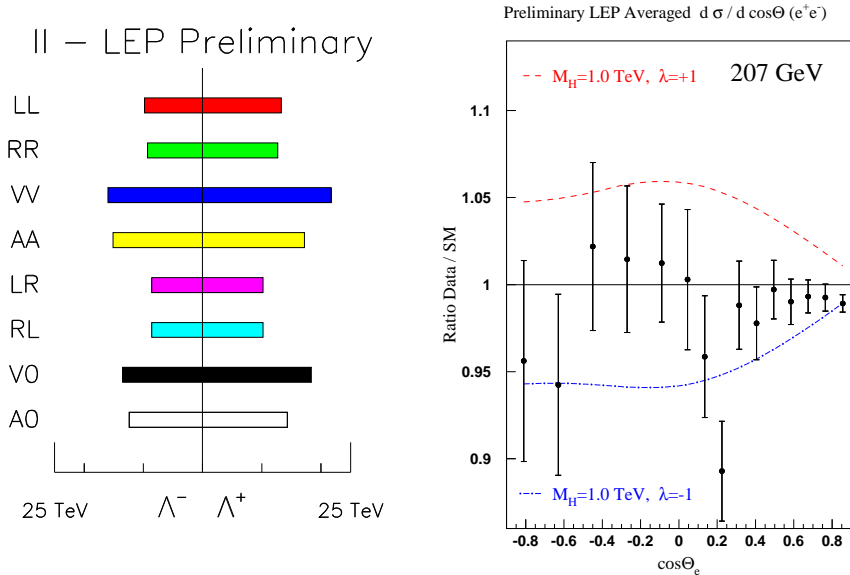


Figure 7: *Left: Examples for limits on contact interactions for μ plus τ final states. Right: Comparison of the e^+e^- final state differential cross-section with the Standard Model expectation and with predictions including virtual graviton exchanges at a mass scale of 1 TeV.*

the Standard Model Z^0 exchange and would thus modify the cross-sections measured at LEP2. The cross-section including the effect of graviton exchange is of the form

$$\frac{d\sigma}{d\cos\theta} = SM + A \cdot \frac{\lambda}{M_H^4} + B \cdot \left(\frac{\lambda}{M_H^4}\right)^2 \quad (7)$$

with a Standard Model term, an interference term and a pure new physics term with an amplitude proportional to λ/M_H^4 (for contact interactions the new physics amplitude is proportional to the inverse of the mass scale squared). The parameter λ , which cannot be known without the knowledge of the full quantum gravity theory, is usually set to ± 1 . Then a fit depending on the parameter $\epsilon = \lambda/M_H^4$ is performed, and a limit on the mass scale M_H , which is related to the new Planck scale M_D , can be derived. At the 95% confidence level, $M_H > 1.20$ TeV (1.09 TeV) for $\lambda = +1$ (-1). So also signs of quantum gravity cannot be seen at LEP2. Figure 7, right, shows the ratio of the measured

differential $e^+e^- \rightarrow e^+e^-$ cross-section at 207 GeV together with the Standard Model expectation. The data are well compatible with 1. The two model predictions for the virtual graviton exchange with a graviton mass of 1 TeV and $\lambda = \pm 1$, however, clearly fail to describe the data.

4 Conclusions and Outlook

The LEP and SLD heavy flavour electroweak measurements have become very stable over the past few years and are almost all finalized. The interpretation in the electroweak Standard Model leads to an interesting discrepancy of 2.9σ between hadronic and leptonic measurements of the effective electroweak mixing angle for leptons, $\sin^2 \theta_{eff}^{lept}$, which is basically due to a discrepancy between the SLD \mathcal{A}_1 and the LEP A_{FB}^b contributions to the average. To discover the origin of this discrepancy will be a task for future colliders.

The measurements of 2-fermion processes at LEP2 energies are in a good overall agreement with the Standard Model expectation. The cross-sections and asymmetries measured by the LEP collaborations are nevertheless used to extract limits on new physics beyond the Standard Model. Models considered include contact interactions, Z' bosons, and low scale gravity. No signs of new physics at LEP are observed. The limits for new physics are mostly well above 1 TeV.

5 Acknowledgements

I would like to thank the LEP/SLD heavy flavour and 2-fermion electroweak working groups for the results presented in this review. In addition, I would like to thank P. Wells, K. Sachs, R. Hawkings and M. Elsing for their critical reading of this text, and the La Thuile conference organizers for their hospitality.

References

1. M. Acciarri *et al.*, Eur. Phys. J. **C13** 47 (2000); G. Abbiendi *et al.*, Eur. Phys. J. **C8** 217 (1999); K. Abe *et al.*, Phys. Rev. Lett. **80** 660 (1998); R. Barate *et al.*, Eur. Phys. J. **C4** 557 (1998); R. Barate *et al.*, Eur. Phys. J. **C16** 597 (2000); P. Abreu *et al.*, Eur. Phys. J. **C12** 209 (2000); P. Abreu *et al.*, Eur. Phys. J. **C12** 225 (2000); K. Ackerstaff *et al.*, Eur. Phys. J. **C1** 439 (1998); G. Alexander *et al.*, Z. Phys. **C72** 1 (1996); SLD Collaboration, paper 174 contributed to ICHEP98 Vancouver, Canada.
2. G. Abbiendi *et al.*, Phys. Lett. **B546** 29 (2002).
3. DELPHI Collaboration, DELPHI-2002-028 CONF 562.

4. M. Acciarri *et al.*, Phys. Lett. **B439** 225 (1998); M. Acciarri *et al.*, Phys. Lett. **B448** 152 (1999); DELPHI Collaboration, DELPHI-2001-048 CONF 476; A. Heister *et al.*, Eur. Phys. J **C22** 201 (2001).
5. P. Abreu *et al.*, Eur. Phys. J. **C10** 219 (1999); G. Alexander *et al.*, Z. Phys. **C73** 379 (1996); A. Heister *et al.*, Eur. Phys. J **C24** 177 (2002); OPAL Collaboration, OPAL Physics Note 226.
6. R. Barate *et al.*, Phys. Lett. **B434** (1998) 415.
7. LEP Electroweak Working Group $f\bar{f}$ Subgroup, LEP2FF/02-03.
8. <http://www.cern.ch/LEPEWWG/lep2/>